# Appendix II

JVI
Journals.ASM.org

# The Human Fetal Glial Cell Line SVG p12 Contains Infectious BK Polyomavirus

**Stian Henriksen,[a] Garth D. Tylden,[a,b] Alexis Dumoulin,[c]* Biswa Nath Sharma,[a,b] Hans H. Hirsch,[c,d] Christine Hanssen Rinaldo[a,e]**

Department of Microbiology and Infection Control, University Hospital of North Norway, Tromsø, Norway[a]; Department of Medical Biology, UiT The Arctic University of Norway, Tromsø, Norway[b]; Transplantation & Clinical Virology, Department of Biomedicine (Haus Petersplatz), University of Basel, Basel, Switzerland[c]; Infectious Diseases & Hospital Epidemiology, University Hospital Basel, Basel, Switzerland[d]; Metabolic and Renal Research Group, UiT The Arctic University of Norway, Tromsø, Norway[e]

**ABSTRACT**

**The human fetal glial cell line SVG was generated in 1985 by transfecting primary fetal brain cells with a plasmid containing an origin-defective mutant of simian virus 40 (SV40). The cells, which express SV40 large T-antigen, support the replication of human JC polyomavirus (JCPyV) and have been used for JCPyV studies but also for other studies in which cells of neural origin were desirable. We intended to use the SVG p12 cells from ATCC for antiviral drug studies with JCPyV. However, during initial experiments, immunofluorescence microscopy controls unexpectedly revealed cells expressing the late viral proteins VP1, VP2/VP3, and agno. This was confirmed by Western blotting. Since our agnoprotein antiserum is specific for BKPyV agnoprotein, infection with BKPyV was suspected. Indeed, specific BKPyV PCR of SVG p12 supernatants revealed a viral load of $>1 \times 10^{10}$ genomic equivalents/ml. Negative-staining electron microscopy showed characteristic polyomavirus virions, and infectious BKPyV was transmitted from SVG p12 supernatant to other cells. Long-range PCR covering the viral genome, followed by DNA sequencing, identified BKPyV strain UT as well as deletion derivatives. This was confirmed by next-generation sequencing. JCPyV (MAD-4) was found to infect apparently uninfected and BKPyV-infected SVG p12 cells. In total, 4 vials from 2 different ATCC lots of SVG p12 cells dating back to 2006 contained BKPyV, whereas the subclone SVG-A was negative. In conclusion, SVG p12 cells from ATCC contain infectious BKPyV. This may have affected results and interpretations of previous studies, and caution should be taken in future experiments.**

**IMPORTANCE**

**This work reveals that one of the most frequently used cell lines for JC polyomavirus (JCPyV) research, the SV40-immortalized human fetal glial cell line SVG p12 obtained directly from ATCC, contains infectious BK polyomavirus (BKPyV) of strain UT and a spectrum of defective mutants. Strain UT has been previously found in urine and in tumors of different patients but is also frequently used for research. It is therefore not clear if BKPyV was present in the brain tissue used to generate the cell line or if this is a contamination. Although productive JCPyV infection of SVG cells was not dependent on prior BKPyV infection, the unnoticed presence of BKPyV may have influenced the results of studies using these cells. The interpretation of past results should therefore be reconsidered and cells tested for BKPyV before new studies are initiated. The frequently used subclone SVG-A did not contain BKPyV and could be a useful substitute.**

The family of human polyomaviruses now includes 12 viruses that seem to at least partly coexist in the human host (1). The first identified and best-studied human polyomaviruses are JC virus (JCPyV) and BK virus (BKPyV) (2, 3). These viruses independently infect most humans early in life and thereafter establish lifelong latent infections in the epithelial cells of the renourinary tract, with occasional reactivation and shedding in urine (4, 5). Although BKPyV and JCPyV infections are usually benign, severe opportunistic diseases may occur in immunocompromised hosts.

JCPyV is the causative agent of progressive multifocal leucoencephalopathy (PML), affecting mainly HIV-positive/AIDS patients, individuals receiving immunomodulatory treatment against autoimmune diseases such as multiple sclerosis, and patients receiving immunosuppressive therapy after organ transplantation (6). BKPyV is the causative agent of polyomavirus-associated nephropathy (PyVAN) in kidney transplant patients and polyomavirus-associated hemorrhagic cystitis (PyVHC) in bone marrow transplant patients (7). Unfortunately, there are currently no effective antiviral drugs against polyomaviruses, and survival is dependent mainly on recovery of polyomavirus-specific immune function.

The viral structure, genome organization, and replication of both JCPyV and BKPyV are closely related to the better-studied monkey polyomavirus simian virus 40 (SV 40). The circular double-stranded DNA genome consists of about 5,200 bp and is arranged in the early viral gene region (EVGR) and late viral gene region (LVGR), separated by a noncoding control region (NCCR) containing the origin of replication, promoters, and enhancer sequences. The EVGR encodes the regulatory proteins small tumor antigen (sTag) and large tumor antigen (LTag) (8). In addition, JCPyV encodes the derivatives T′135, T′136, and T′165 (9), while

**Received** 9 March 2014 **Accepted** 14 April 2014
**Published ahead of print** 23 April 2014
**Editor:** M. J. Imperiale
Address correspondence to Christine Hanssen Rinaldo, christine.rinaldo@unn.no.
* Present address: Alexis Dumoulin, Division of Infectious Diseases, Central Institute, Valais Hospital, Sion, Switzerland.

doi:10.1128/JVI.00696-14

BKPyV encodes TruncTag (10). LTag plays a pivotal role in viral genome replication, transcription, and virion assembly (11). Presumably, LTag also optimizes the conditions for viral replication by interacting with p53 and pRb family proteins, thus preventing growth arrest and apoptosis and facilitating expression of E2F-dependent growth-inducing genes, driving resting host cells into the cell cycle (11, 12). The LVGR encodes the nonstructural agnoprotein and the viral capsid proteins 1, 2, and 3 (VP1 to VP3) forming the icosahedral capsid.

Animal models to study JCPyV and BKPyV replication and disease have been missing. Only recently, mice with human thymus and lymphocytes were generated to study the JCPyV-specific immune responses (13). During PyVAN and PyVHC, BKPyV replicates extensively in renal tubular epithelial cells and bladder epithelial cells, respectively (14). Primary cultures of these cells provide good model systems for *in vitro* studies of BKPyV replication (15–17). In addition, BKPyV can successfully replicate in a large variety of cells or cell lines. In contrast, JCPyV is more difficult to propagate and an authentic cellular model system is lacking (6). The main cause of PML pathology is JCPyV infection of oligodendrocytes; however, oligodendrocytes are difficult to culture unless they are immortalized. Astrocytes may possibly be infected via direct contact with internalized JCPyV-infected oligodendrocytes (18). Recently, 293TT cells that constitutively express simian virus 40 (SV40) LTag were found to support replication of archetype JCPyV (19). These cells were originally derived from a human embryonic kidney but are probably of neuronal linage (20).

The SV40-immortalized glial cell line SVG was originally developed as a model system facilitating research on JCPyV replication. The cell line was derived from human fetal glial cells immortalized with a plasmid conferring constitutive SV40 LTag expression (21, 22). The SV40 strain used contained a deletion in the origin of replication that affected two of the three LTag binding sites, thus preventing replication of the SV40 genome.

Based on the expression of glial fibrillary acidic protein (GFAP) and lack of the myelin marker galactocerebroside (GC), the cell line was originally characterized as an astrocyte cell line (21). However, the cells' ability to increase expression of GFAP and to synthesize GC when the appropriate growth signals were present caused speculations that the cells were neural progenitor cells with the potential to differentiate (23). This speculation was supported by the apparent lack of estrogen receptor alpha (ERα) expression, which is usually found in astrocytes (24, 25), and also by their undifferentiated epithelial phenotype when grown in minimal essential medium supplemented with 10% fetal bovine serum (FBS) (23).

The cell line designated SVG p12, although the passage number is said to be unknown, has been provided by the ATCC since 1987. SVG p12, SVG, and subclones of SVG have been used in several JCPyV studies (26–41) and in more than 30 other studies in which cells of neural origin were required. Unfortunately, the source of the SVG cells was not clearly specified for some of these studies.

Here we report our unexpected finding that a subpopulation of SVG p12 cells, obtained directly from ATCC, is productively infected with BKPyV. This stowaway virus may have influenced research performed in these cells and should be considered in the interpretation of past results and in future experiments.

## MATERIALS AND METHODS

**Cells and virus.** Human fetal glial (SVG p12) cells (ATCC CRL-8621 [www.atcc.org]) were cultured in minimum essential Eagle medium (M4655; Sigma-Aldrich) containing 10% FBS. African green monkey kidney epithelial (Vero) cells (ATCC CCL-81) were cultured in Dulbecco's modified Eagle's medium (D5671; Sigma-Aldrich) with 10% FBS and 1× GlutaMax-I (catalog number 35050; Invitrogen). SV40-transformed African green monkey kidney fibroblast (COS-7) cells (ATCC CRL-1651) were cultured in Dulbecco's modified Eagle's medium with 5% FBS and 1× GlutaMax-I. A subclone of SVG, SVG-A (42), was kindly provided by Walter Atwood, Brown University, and cultured in minimum essential Eagle medium (M4655; Sigma-Aldrich) containing 10% FBS.

Human renal proximal tubular epithelial cells (RPTECs; ScienCell Research Laboratories) were cultured in renal epithelial growth medium (REGM; Lonza) containing 0.5% FBS. All experiments were performed with RPTECs at passage 4.

Infectious JCPyV (MAD-4) (ATCC VR-1583) supernatants obtained from COS-7 cells and infectious BKPyV (Dunlop) (ATCC 45025) supernatants obtained from Vero cells were used for infection and as PCR controls.

**Viral infection.** Supernatants from SVG p12 cells were used to infect RPTECs and Vero cells. As a positive control, BKPyV (Dunlop) supernatant was used. SVG p12 cells were infected with JCPyV (MAD-4), and SVG-A cells were infected with BKPyV (Dunlop). All infections were carried out for 2 h before surplus infectious units were removed, cells were washed once with phosphate-buffered saline (PBS), and complete medium was added.

**Immunofluorescence staining, microscopy, and digital image processing.** Immunofluorescence staining was performed as previously described (43). The following primary antibodies were used: polyclonal rabbit antisera directed against SV40 VP1 (ab53977; Abcam), SV40 VP2 + VP3 (ab53983; Abcam), and BKPyV agnoprotein (44, 45); two mouse monoclonal antibodies directed against SV40 LTag (Pab 416; Abcam; and Pab 419; Santa Cruz Biotechnology); and a mouse monoclonal antibody directed against JCPyV VP1 (ab34756; Abcam). While ab53977, ab53983, and Pab 416 all cross-react with BKPyV proteins, the agnoprotein antiserum recognizes only BKPyV agnoprotein, ab34756 recognizes JCPyV VP1 but not BKPyV VP1, and Pab 419 recognizes only SV40 LTag. As secondary antibodies, a combination of anti-mouse antibody conjugated with Alexa Fluor 568 (1:500; Molecular Probes) and anti-rabbit antibody conjugated with Alexa Fluor 488 (1:500; Molecular Probes) was used. Nuclei were stained with Draq5 (Biostatus). Images were captured using a Zeiss Axiovert 200 confocal microscope equipped with an LSM510-Meta confocal module using the LSM5 software version 3.2 (Carl Zeiss).

**Western blotting.** SVG p12 cells cultured for 4 days in a 25-$cm^2$ flask were lysed in 1.5 ml of radioimmunoprecipitation assay buffer (150 mM sodium chloride, 1% Nonidet P-40, 0.5% sodium deoxycholate, 0.1% sodium dodecyl sulfate, 50 mM Tris, pH 8.0), collected, and stored at −70°C. Next, total protein was measured using the EZQ protein quantitation kit (Invitrogen) according to the manufacturer's instructions using a microplate reader (Infinite F200 Pro; Tecan). Cell lysates containing 7.2 μg of total protein were separated by electrophoresis on a NuPAGE 4 to 12% Bis-Tris gel (Invitrogen) and blotted onto a PVDF (polyvinylidene fluoride) membrane (LI-Cor Biosciences). The membrane was blocked with Odyssey blocking buffer (LI-Cor Biosciences) and incubated with the following primary antibodies: polyclonal rabbit antisera directed against BKPyV VP1 (46) and BKPyV agnoprotein (44, 45) and two different monoclonal antibodies directed against SV40 LTag (Pab 416 from Abcam and Pab 419 from Santa Cruz). In addition, a monoclonal mouse antibody directed against the housekeeping protein glyceraldehyde-3-phosphate dehydrogenase (GAPDH) (ab8245; Abcam) was used. As secondary antibody, a combination of IRDye 800CW goat anti-rabbit antibody (LI-Cor Biosciences) and IRDye 680RD goat anti-mouse antibody (LI-Cor Biosciences) was used before detection with the LI-Cor Odyssey infrared detection system.

**Quantification of extracellular and intracellular BKPyV load.** Extracellular BKPyV DNA determined by quantitative PCR (qPCR) of supernatants using primers and a probe targeting the BKPyV LTag gene (47). Supernatants were diluted in molecular grade water (1:100; Lonza) and boiled for 5 min. Five microliters was used for a 25-μl PCR mixture. Intracellular BKPyV DNA load was determined by performing the same qPCR on DNA extracted from cells using the GenoM-48 platform (GenoVision) with MagAttract DNA mini-M48 kit (Qiagen catalog number 953336) or the QIAsymphony (Qiagen).

**Negative-staining electron microscopy.** Supernatants collected from SVG p12 cells 4 days after seeding were ultracentrifuged in Beckmann ultraclear tubes (40 ml) in an SW28 rotor at 28,000 rpm for 90 min at 4°C. The supernatant was removed, and the pellet was dissolved in 1 ml $H_2O$. As a positive control, supernatants from Vero cells 3 weeks postinfection with BKPyV Dunlop were processed in parallel. The pellet suspensions were fixed with 2% paraformaldehyde (PFA), and negative staining was performed. In short, 10 μl of virus suspension was deposited on carbon-coated copper grids and air dried for 5 min before 10 μl of 3% uranyl acetate was added and a 15-min final air drying was performed. The grids were examined in a JEOL JEM 1010 transmission electron microscope (JEOL, Tokyo, Japan) operating at 80 kV.

**Long-range PCR.** Supernatants from SVG p12 cells or from RPTECs inoculated with SVG p12 supernatant were harvested and prepared for long-range PCR as previously described for qPCR. Long-range PCR was performed with partly overlapping primers targeting the VP1 gene (adapted from reference 48) and a high-fidelity Phusion polymerase (New England BioLabs M0530S) according to the manufacturer's instructions. Briefly, a reaction volume of 50 μl was used, consisting of 10 μl 5× Phusion HF buffer, 1 μl deoxynucleoside triphosphate (dNTP) mix (10 mM), 1 μl of each of the primers Eco-F and Eco-R (10 μM) (Table 1), 0.5 μl Phusion HF polymerase, 5 μl of the diluted supernatants, and $H_2O$ for the remainder. The cycling program started with initial denaturing at 98°C for 30 s followed by 35 cycles of 98°C for 10 s, 70°C for 30 s, and 72°C for 2.5 min and finishing with elongation at 72°C for 10 min. The annealing temperature (AT) of 70°C was set based on melting temperature ($T_m$) calculations using the New England BioLabs $T_m$ calculator. Five microliters of the PCR product was run on a 0.8% agarose gel at 110 V for 400 min and visualized with GelRed (Biotium) using the GelDoc XR gel imager (Bio-Rad). The remaining 45 μl of the PCR product was purified using the NucleoSpin Gel and PCR Cleanup kit (Macherey-Nagel Gmbh) according to the manufacturer's instructions and stored at 4°C until sequencing or cloning.

**Cloning of long-range PCR products.** The long-range PCR products were prepared for TA cloning using the TOPO XL PCR cloning kit (K7030-20; Invitrogen). A 3′adenine overhang was created by adding 0.2 μl dATP and 0.5 μl *Taq* polymerase (both from Sigma-Aldrich) to 20 μl of the PCR product and incubating the mixture in a thermocycler at 72°C for 10 min. The PCR product was purified using the NucleoSpin Gel and PCR Cleanup kit (Macherey-Nagel Gmbh), and 4 μl of the purified PCR product was used for TA cloning according to the manufacturer's instructions. Plasmids from 10 colonies were purified using the PureLink Quick Plasmid Miniprep kit (Invitrogen), and the presence of inserts was confirmed by restriction enzyme digestion with EcoRI (New England BioLabs) followed by agarose gel electrophoresis.

**Conventional DNA sequencing.** Sanger sequencing of the whole genome of BKPyV was accomplished using 20 primers with binding sites dispersed along both strands of the genome of BKPyV (Table 1), while shorter inserts were sequenced using M13R and T7 primers (Table 1). The BigDye v3.1 sequencing kit (Applied Biosystems) was used according to the manufacturer's instructions. The products of the sequencing reactions were analyzed by capillary electrophoresis at the DNA sequencing core facility at the University Hospital of North Norway. Sequences were analyzed using the Geneious software version 6.1.3 (Biomatters).

**DNA preparation and rolling-circle amplification.** Supernatant from SVG p12 culture was centrifuged twice at 1,000 relative centrifugal force (RCF) for 15 min. DNA was then extracted from 200 μl supernatant using the QiaSymphony SP and DNA minikit (Qiagen, Hilden, Germany), generating 100 μl DNA extract with a BKPyV DNA load of $4.7 \times 10^9$ genomic equivalents (GEq)/ml. Rolling-circle amplification was performed using 0.5 μl of the DNA and the TempliPhi 100 amplification kit (GE Healthcare Lifescience) according to the instructions of the manufacturer. A nontemplate control was processed in parallel to ensure the specificity of the sequencing. The concentration of the amplified DNA was determined using the PicoGreen system (Invitrogen). An amount of 500 ng was processed further for the library preparation.

**Next-generation sequencing (NGS).** The TemphiPhi-amplified DNAs from the supernatant and the nontemplate control were fragmented by nebulization, using the Roche GS Titanium Rapid Library Preparation kit (454 Life Science/Roche) according to the manufacturer's instructions. The libraries were labeled with different multiplex identifiers (MID) and processed together. Briefly, the combined libraries were amplified by emulsion PCR and the clonally amplified DNA molecules were enriched and purified using the Roche GS Junior Titanium emPCR kit according to the manufacturer's instructions. Finally, the enriched fragments were sequenced on the Roche GS Junior instrument, using the Roche GS Junior Titanium sequencing kit.

**NGS data analysis: mapping and *de novo* assembly.** The reads of the SVG p12 library were analyzed in groups of a maximum of 4,000 reads using the Roche GS Reference mapper software (version 2.7) and the CLC Genomics Workbench for *de novo* assembly (version 6.0.3). The obtained contigs were compared to the NCBI sequence database using the BLAST algorithm.

## RESULTS

**SVG p12 cells from ATCC are infected with BKPyV.** The SVG p12 cells are transformed with a plasmid containing an origin-deficient SV40 genome, and all cells are therefore supposed to express SV40 LTag (21). As an initial characterization of the cells before JCPyV infections and antiviral studies, immunofluorescence staining was performed with two different monoclonal antibodies directed against SV40 LTag (Pab 416 and Pab 419) and two polyclonal antisera directed against the N- and C-terminal part of BKPyV LTag (81048 and 81178) (44) also known to cross-react with SV40 LTag. As expected, immunofluorescence microscopy revealed nuclear LTag expression in all cells, and this was independent of the different LTag antibodies used (Fig. 1A, Pab 419; Fig. 1B, Pab 416; for 81048 and 81178, data not shown). The staining was very strong in some cells but weaker in others.

Considering the possibility that the origin-deficient plasmid originally used to transform the SVG p12 cell line could give rise to SV40 late proteins and to exclude nonspecific staining with other potentially useful antibodies, we included antibodies and antisera directed against SV40, JCPyV, and BKPyV late proteins in our initial characterization. Surprisingly, a small subpopulation of cells stained positive for VP1 (Fig. 1A) as well as VP2/VP3 (results not shown). Even more unexpectedly, immunofluorescence with an anti-BKPyV agnoserum stained a subpopulation of the cells (Fig. 1B). While the SV40 VP1 and VP2/VP3 antisera are known to cross-react with BKPyV and JCPyV proteins and therefore did not identify the virus involved, the rabbit polyclonal agnoprotein antiserum is specific for BKPyV agnoprotein and, in our experience, does not cross-react with either SV40 agnoprotein or JCPyV agnoprotein (S. Sørensen, B. N. Sharma, and C. H. Rinaldo, unpublished data). The positive agnoprotein staining therefore suggested the presence of BKPyV in the SVG p12 cells.

In order to confirm the expression of BKPyV agnoprotein and VP1 and at the same time confirm the expression of SV40 LTag, Western blotting was performed on SVG p12 cell extracts. As a

**TABLE 1** Primers and PCR conditions

| Application, name, and condition | 5′–3′ sequence | Reference or source |
|---|---|---|
| BKPyV sequencing | | |
| BK345F | CTAGGAATCTTGGCCTTGTCCCC | 77 |
| BK831F | GTAATTGCTGGTGCTCCTGGGGC | 77 |
| BK1319F | AGTAGCTGAAAGGGAAGGTACCCG | 77 |
| BK1731F | GGGGGATCCAGATGAAAACCTTAGGGGCTTTAG | 77 |
| BK2217F | TGCTAGGTATTTTGGGACTTTCACA | 77 |
| BK2723F | TATTTTGGGGGTGGTGTTTTAGGCC | 77 |
| BK3216F | CATTCATTGTAACCAAGCCTGGTGG | 77 |
| BK3712F | TCTTTCTGTTAGCATTTCTTCCCTGG | 77 |
| BK4075F | GTATGGTATGGATCTCTAGTTAAGGC | 77 |
| BK4857F | AGGCCATTCCTTGCAGTACAGGG | 77 |
| BK740R | TTCTATAGCAGCAGCAGCCTCCCC | 77 |
| BK1223R | AGTTTCCTCCAAAAATCTAGCCAAGG | 77 |
| BK1739R | GGATCCCCCATTTCTGGGTTTAGGAAGCATTCTAC | 77 |
| BK2213R | TCATTTCTACTGGGATCAGGTACCC | 77 |
| BK2715R | CTTAAAAGTGGCTTATACAAAAGCAGC | 77 |
| BK3184R | ATTTGTAAGACAAATAGATTTTAGGCCC | 77 |
| BK3632R | TTGCTTGGCTGCACTGTTTG | |
| BK4076R | CTATAGAAGAAAGCATTCAAGGGGGC | 77 |
| BK4461R | GAAGCAACAGCAGATTCTCAACACTCAACACCACCC | 77 |
| LTag32f | TCCATGGAGCTCATGGACCTTT | |
| M13R | CAGGAAACAGCTATGAC | TOPO XL PCR Cloning kit (Invitrogen) |
| T7 | TAATACGACTCACTATAGGG | |
| Quantitative PCR | | |
| BK-Deg2-Forward | AGCAGGCAAGDGTTCTATTACTAAAT | 47 |
| BK-Deg-Reverse | GARGCAACAGCAGATTCYCAACA | 47 |
| BK-Deg-Probe | 6-FAM-AAGACCCTAAAGACTTTCCYTCTGATCTACACCAGTTT- 6-Tamra | 47 |
| Long-range PCR (AT, 70°C; 35 cycles; high-fidelity Phusion polymerase [NEB]) | | |
| Eco-F | CAAGAATTCCCCTCCCCAATTTAAATG | Adapted from reference 48 |
| Eco-R | GGGGAATTCTTGCTGTGCTGTAAC | Adapted from reference 48 |
| NCCR PCR (AT, 55°C; 30 cycles) | | |
| GPPY1 | CCAAAATCAGGCTGATGAGC | 78 |
| GPPY2 | TTCCCGTCTACACTGTCTTC | 78 |
| BKPyV LVGR PCR (AT, 55°C; 30 cycles) | | |
| BKPA1 | TACTACTTGAGAGAAAGGGTGGA | 49 |
| BK1739R | GGATCCCCCATTTCTGGGTTTAGGAAGCATTCTAC | 77 |
| BKPyV EVGR PCR (AT, 63°C; 30 cycles) | | |
| O-block | CTCTGCCTCCACCCTTTCTCTCAAG | |
| VP1 C-term | AGACTTCCAGGGGACCCAGATATG | |

positive control for LTag expression, cell extracts from COS-7 were included, while cell extracts from Vero cells were used as a negative control for LTag expression and BKPyV infection. The results confirmed that SVG p12 expressed BKPyV agnoprotein (~7 kDa) as well as VP1 (40 kDa) and, as anticipated, LTag (80 kDa) (Fig. 1C). As expected, COS-7 cells expressed only LTag, whereas uninfected Vero cells did not express any of the targeted PyV proteins (Fig. 1C).

To test for the presence of BKPyV DNA, supernatants from SVG p12 cells were analyzed 4 days postseeding by a BKPyV-specific quantitative real-time PCR (qPCR). A viral DNA load of $>1 \times 10^{10}$ GEq/ml was found, demonstrating the presence BKPyV DNA in the supernatant.

To exclude the possibility that the cells or assays had been contaminated in the lab in Tromsø, a new vial of SVG p12 cells with a different lot number was ordered from ATCC and tested directly in the accredited diagnostic laboratory in Basel. Again, BKPyV proteins were detected by immunofluorescence staining and extracellular BKPyV DNA found by qPCR (results not shown). According to the data sheet, the first lot of SVG p12 cells had been cryopreserved at ATCC in 2006, while the new lot was cryopreserved in 2010. Therefore, a third order of the second lot was

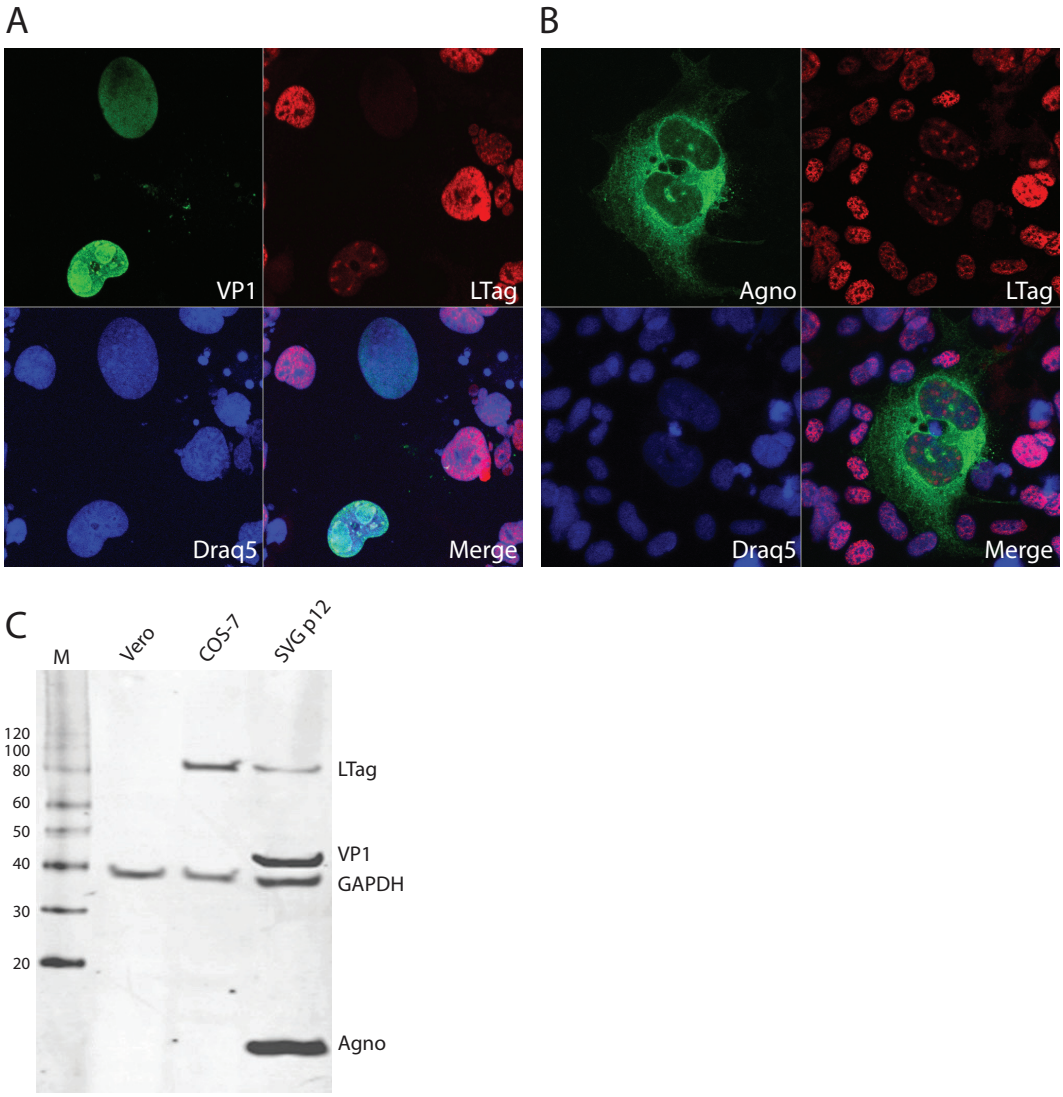


**FIG 1** The SVG p12 cell line expresses BKPyV late proteins. SVG p12 cells were fixed 4 days postseeding, and indirect immunofluorescence staining was performed using different combinations of primary antibodies: SV40 VP1 rabbit polyclonal antiserum (green, Alexa Fluor 488) with the SV40-specific LTag mouse monoclonal antibody Pab419 (red, Alexa Fluor 568) (A); and BKPyV agnoprotein rabbit polyclonal antiserum (green, Alexa 488) with SV40 LTag mouse monoclonal antibody Pab416 (red, Alexa Fluor 568) (B). The DNA (nucleus) was stained with Draq5 (blue), and both images were acquired by confocal microscopy with a 40× objective. (C) Western blot of cell lysate (7.2 μg protein/lane) from Vero, COS-7, and SVG p12 cells 4 days postseeding. The membrane was labeled with SV40 LTag mouse monoclonal antibody, Pab 416, BKPyV VP1 rabbit polyclonal antiserum, BKPyV agnoprotein rabbit polyclonal antiserum, and anti-GAPDH mouse monoclonal antibody. M, molecular weight marker (MagicMark XP Western standard; Invitrogen).

processed directly for DNA extraction and BKPyV qPCR in the laboratory in Basel, and a fourth order of the same lot was processed directly for DNA extraction and BKPyV qPCR in the accredited diagnostic laboratory in Tromsø. The results showed that both vials contained more than $1 \times 10^{10}$ GEq/ml BKPyV, further confirming that the SVG p12 cells stored at ATCC were infected with BKPyV. Apparently, BKPyV has been present in these cells since 2006 or earlier.

**SVG p12 cultures produce infectious BKPyV.** Given the high BKPyV genome viral load in supernatants from SVG p12 cells, we next investigated whether or not viral particles were released. Supernatants from SVG p12 cells were harvested at 4 days postseeding, enriched by ultracentrifugation, and used for negative-staining electron microscopy. As a positive control, a supernatant from BKPyV (Dunlop)-infected Vero cells was used. The negative staining revealed numerous viral particles with a diameter of about 40 to 50 nm and small surface projections characteristic of polyomavirus capsomers (Fig. 2A). Similar viral particles were found in supernatants from BKPyV-infected Vero cells (result not shown).

To investigate whether the virus released from the SVG p12 cell line consisted of infectious BKPyV, SVG p12 cell supernatants were used to infect RPTECs and Vero cells. Vero cells are known to be semipermissive, while RPTECs are highly susceptible to BKPyV (15, 49). Cells were fixed at 3 days postinfection (dpi), and immunofluorescence staining was performed with primary antibodies directed against BKPyV agnoprotein and SV40 LTag. Microscopy clearly demonstrated infection of RPTECs (Fig. 2B) expressing

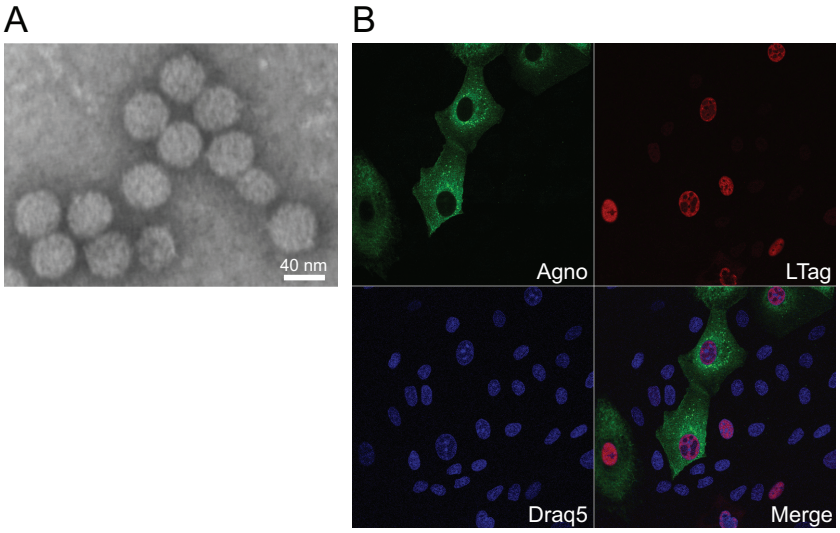


**FIG 2** The SVG p12 cell line produces infectious BKPyV. (A) Electron microscopy of negatively stained viral particles from supernatant harvested from SVG p12 cells 4 days postseeding. (B) Immunofluorescence staining of RPTECs 3 days following exposure to supernatant harvested from SVG p12 cells 4 days postseeding. Indirect immunofluorescence staining was performed using a combination of BKPyV agnoprotein rabbit polyclonal antiserum (green, Alexa Fluor 488) and SV40 LTag mouse monoclonal antibody, Pab 416 (red, Alexa Fluor 568). The DNA (nucleus) was stained with Draq5 (blue). Images were acquired by confocal microscopy with a 40× objective.

only LTag or LTag and agnoprotein. Similar results were obtained for Vero cells (data not shown). The results demonstrate that SVG p12 cells were infected by BKPyV and produced infectious BKPyV capable of initiating infection in RPTECs and Vero cells.

**SVG p12 cultures contain a mixture of complete and defective BKPyV UT genomes.** To genetically characterize the BKPyV strain infecting the SVG p12 cell line, the NCCR was amplified by PCR and sequenced. The cells were found to contain BKPyV of strain UT. The NCCR of strain UT was detected by PCR of urine samples of patients in North Norway for the first time in 1990 but was then designated TU (50) (GenBank M34049). In 2005, the complete genome of a virus with an identical NCCR, apparently an isolate from the urine of a patient in the United States with a solid tumor, was submitted to the GenBank and named strain UT (GenBank DQ305492) (51). The UT NCCR lacks a full R-block and contains a partly duplicated P-block, Q-block, and R-block. Compared to the GenBank sequences, only one nucleotide was missing in the O-block (nt 127).

To characterize the full-length genome, a long-range PCR using a high-fidelity polymerase was performed on SVG p12 cell supernatants. As a positive control, a supernatant from BKPyV Dunlop-infected RPTECs was used. Agarose gel electrophoresis revealed several PCR products with sizes of around 1,200 bp, considerably lower than the expected ~5,000-bp BKPyV genome (Fig. 3A, 4 days).

We reasoned that the full genome was not well amplified due to low copy numbers. In order to increase the likelihood of detecting full-length genomes, the SVG p12 cells were seeded and maintained in culture for 58 days and the long-range PCR was repeated. This time, a weak band corresponding to the whole genome was obtained, again together with several other smaller bands, making the PCR product unsuitable for whole-genome cloning (Fig. 3A, 58 days).

We therefore hypothesized that infection of more-permissive cells would favor the production of virus and thereby enrich for the complete BKPyV genome. A supernatant from SVG p12 cells was therefore passaged twice on RPTECs, each time for 6 days, before supernatant was harvested and long-range PCR performed. A supernatant from BKPyV (Dunlop)-infected RPTECs was used as a positive control. This time, agarose gel electrophoresis revealed one strong band with the expected size of the BKPyV genome (Fig. 3B). The complete PCR product was DNA sequenced by the Sanger method using 20 primers producing overlapping sequences. The sequencing revealed that the 5,189-bp genome amplified from SVG p12 supernatants was almost identical to the BKPyV UT genome (GenBank DQ305492) with the exception of the previously mentioned nucleotide missing in the O-block (nt 127) and a point mutation in the intergenic region between agnoprotein and VP2 (nt 629, A-to-G transition).

We also investigated the identity of the smaller-size bands detected by long-range PCR directly on supernatants from SVG p12 cells. To reduce the chance that this was nonspecific amplification of cellular DNA or partly degraded free viral DNA released from dead cells, DNase treatment of the cell supernatant was performed prior to long-range PCR. However, the approach failed to remove the smaller-size bands, thereby suggesting that the DNA was encapsidated or otherwise protected (data not shown). A TA cloning of the heterogeneous PCR product was therefore performed. PCR of 10 colonies using primers in the TA vector revealed inserts ranging from approximately 300 bp to 2,000 bp. The inserts were sequenced with the Sanger method, and all were found to contain BKPyV DNA in fragments ranging from 100 bp to about 900 bp (Fig. 3C). Three of the 10 clones also contained part of or the complete previously identified UT NCCR. The subgenomic fragments covered less than 50% of the BKPyV UT genome and included different parts of the genome. This suggested a population of highly fragmented genomes.

To further investigate the presence of BKPyV genome fragments in the SVG p12 cell supernatant, we also performed two separate PCRs targeting the EVGR and a large part of the LVGR

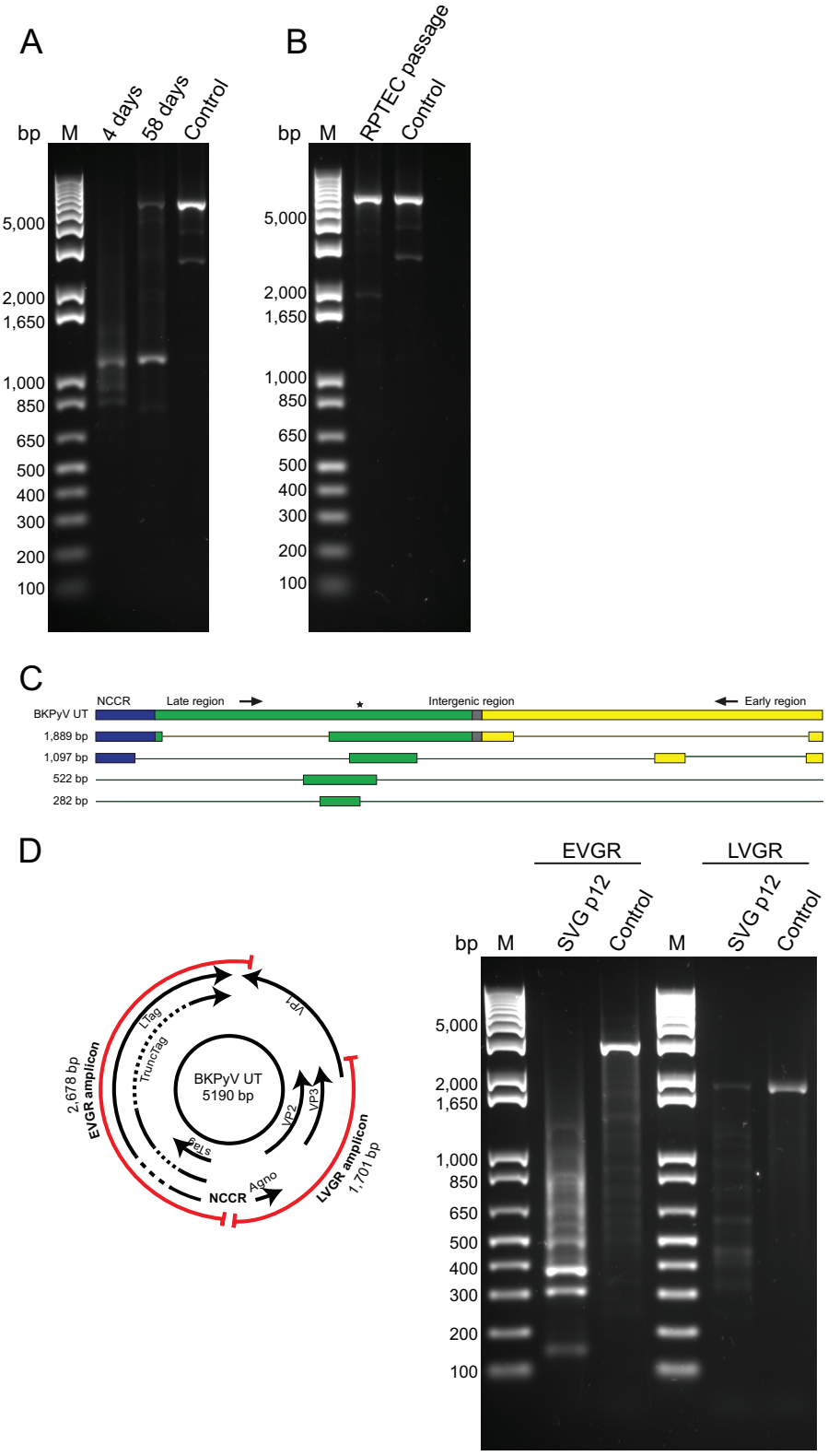


**FIG 3** The BKPyV DNA isolated from the SVG p12 cell line consisted of a mixture of complete and defective genomes. (A) PCR products generated from long-range PCR of SVG p12 supernatants 4 days postseeding and 58 days postseeding were separated on a 0.8% agarose gel. A supernatant harvested from BKPyV-infected RPTECs 3 days postinfection was included as a positive control. (B) PCR products generated from long-range PCR of RPTEC supernatant after infection with an SVG p12 supernatant (the virus was passaged twice in RPTECs). A supernatant harvested from BKPyV-infected RPTECs 3 days postinfection was included as a positive control. (C) Defective genomes detected by long-range PCR followed by TA cloning and Sanger sequencing. The different regions of the genome are color coded: NCCR, blue; LVGR, green; intergenic region, gray; EVGR, yellow. Deletions are indicated by a thin line. The star indicates the binding sites of the partly overlapping primers used for long-range PCR. (D) Schematic display of the BKPyV UT genome with the different reading frames annotated and with the PCR-amplified regions marked in red and subsequent PCR products from EVGR and LVGR, respectively, separated on a 1% agarose gel. PCR product from the BKPyV Dunlop plasmid served as a positive control. M, 1 Kb Plus DNA ladder (Invitrogen).

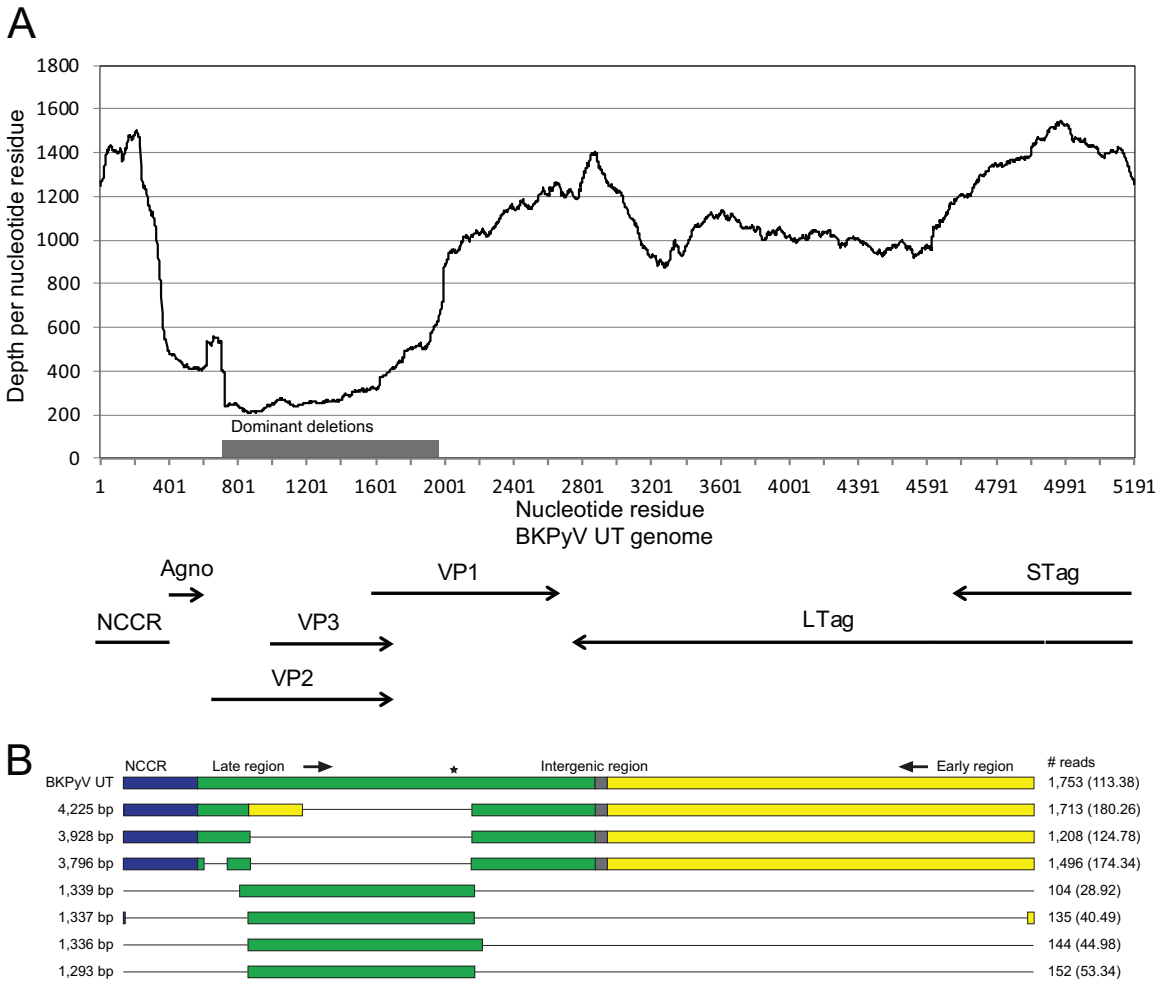


**FIG 4** The BKPyV DNA isolated from the SVG p12 cell line consisted of a mixture of complete and defective genomes as detected by NGS. (A) Coverage per nucleotide of the 454 reads when aligned to the BKV UT genome. The positions of the dominant deletion as well as the BKPyV open reading frames are indicated. (B) Some defective genomes detected by NGS. Numbers of reads are indicated next to the defective genomes, and the average coverage is given in parentheses. The different regions of the genome are color coded: NCCR, blue; LVGR, green; intergenic region, gray; EVGR, yellow. Deletions are indicated by a thin line. The star indicates the binding sites of the partly overlapping primers used for long-range PCR.

(Fig. 3D) (primers and PCR conditions are shown in Table 1). Agarose gel electrophoresis of the PCR products revealed several bands migrating faster than the strong and distinct bands in the positive control (Fig. 3D). Since these results were obtained with primers different from those used for long-range PCR, they supported our finding of highly fragmented BKPyV genomes in SVG p12 cell supernatants.

In order to validate these results in an independent manner, next-generation sequencing (NGS) was performed after rolling-circle amplification of DNA extracted from SVG p12 supernatants. A total of 70,818 reads were obtained, including 22,610 for the SVG p12 library and 43,855 for the nontemplate control library. The median read length was 496 nucleotides (range, 40 to 733) with an average quality score of 37.05 (standard deviation, 7.79). None of the reads of the nontemplate control library could be matched to the BKPyV reference, excluding contaminating DNA. The *de novo* assembly of the SVG p12 reads yielded a contig of 5,182 bp (1,753 reads; average depth, 113.38), with 8 mismatches to the BKPyV strain UT (GenBank DQ305492) (Fig. 4A). All mismatches were located in homopolymer stretches, a common artifact of pyrosequencing. Interestingly, the *de novo* assembly also resulted in several contigs containing deletions in the VP2-VP3-VP1 region, ranging from nucleotides 720 to 1990 (Fig. 4A and B). A total of 10,350 reads (45.3%) of the SVG p12 library could be mapped to the BKPyV UT genome. Of those, 85 reads contained both ends of the deletion, confirming that this extended from residue 720 to residue 1990. Moreover, the depth of the NGS reads was strongly reduced in the agno-VP2-VP3-VP1 region compared to the rest of the genome, suggesting that variants with a deletion in this area were dominant (Fig. 4A).

Thus, SVG p12 cells were productively infected by BKPyV UT but also produced circular subgenomic DNA fragments that seemed to be encapsidated. Passage of infectious units in RPTECs appeared to select for full-length genomes, suggesting that virions with fragmented genomes are not infectious or are less fit than BKPyV UT, at least in RPTECs.

**SVG p12 cells with and without BKPyV late protein expression can be infected by JCPyV.** Since SVG p12 cells have been used in at least two published JCPyV studies (32, 39), it cannot be

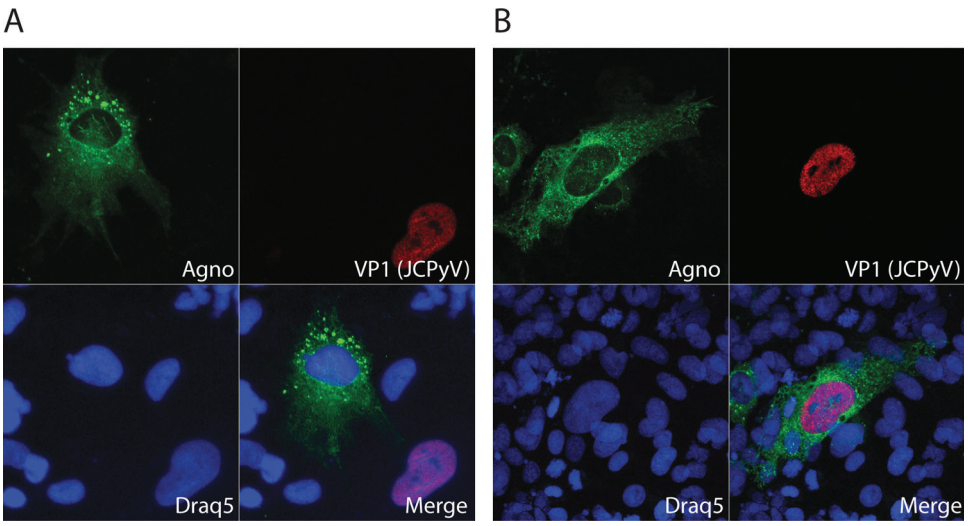


**FIG 5** JCPyV can infect SVG p12 cells both with and without BKPyV late protein expression. SVG p12 cells were infected with JCPyV, and indirect immunofluorescence staining was performed 4 days postinfection using a combination of the BKPyV-specific agnoprotein rabbit polyclonal antiserum (green, Alexa Fluor 488) and the JCPyV-specific JCPyV VP1 mouse monoclonal antibody (red, Alexa Fluor 568). The DNA (nucleus) was stained with Draq5 (blue). Images were acquired by confocal microscopy with a 40× objective. Cells were either infected with BKPyV or JCPyV (A) or coinfected with BKPyV and JCPyV (B).

excluded that these studies were unknowingly performed with BKPyV present. In order to find out if JCPyV infection in SVG p12 requires coinfection with BKPyV, SVG p12 cells were infected with JCPyV (MAD-4). The cells were fixed 4 dpi, and JCPyV- and BKPyV-infected cells were identified by immunofluorescence staining using a combination of a monoclonal antibody specific for JCPyV VP1 and the polyclonal BKPyV agnoprotein antiserum specific for BKPyV-infected cells. Microscopy revealed that, overall, a low number of SVG p12 cells were infected with either of the viruses (Fig. 5A). However, some cells were clearly coinfected with JCPyV and BKPyV (Fig. 5B).

Thus, SVG p12 cells seem to be able to support the JCPyV life cycle in parallel to and independently of detectable BKPyV infection. However, coinfections of cells with JCPyV and BKPyV do also occur.

**The SVG-A cell line, a frequently used subclone of SVG cells, does not contain BKPyV.** Based on these results, the question arose whether or not the SVG-A cell line established by limiting dilution assay of SVG cells (42) and commonly used for JCPyV studies (29–31, 33, 37, 41, 52–55) was also harboring BKPyV. A supernatant harvested from SVG-A cells at 4 days postseeding was subjected to BKPyV qPCR. Intracellular DNA was also extracted and subjected to BKPyV qPCR. In addition, immunofluorescence staining with several late protein antibodies was performed. The supernatant and intracellular DNAs were both negative for BKPyV DNA, and the cells expressed only SV40 LTag (Fig. 6A).

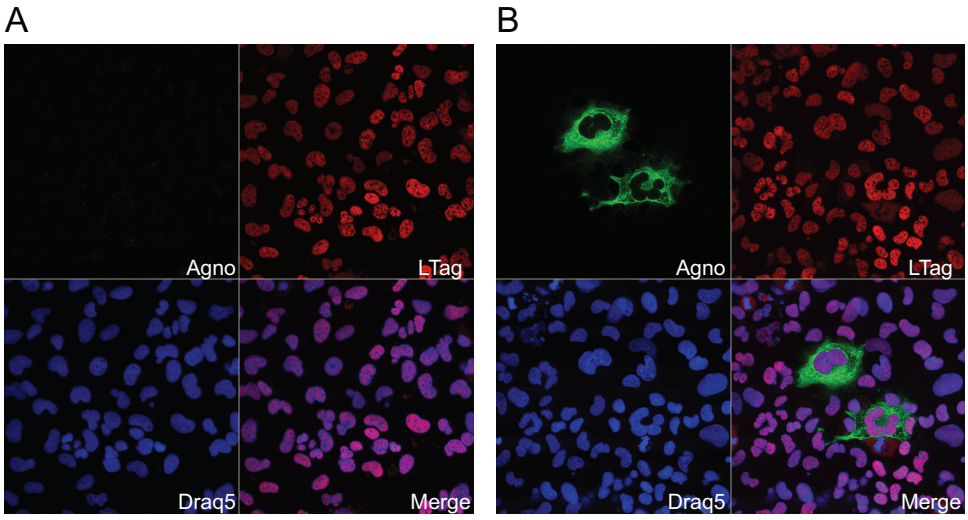


**FIG 6** SVG-A cells do not express BKPyV late proteins inherently but are permissive for BKPyV infection. Indirect immunofluorescence staining of SVG-A cells was performed using a combination of BKPyV agnoprotein rabbit polyclonal antiserum (green, Alexa Fluor 488) and SV40 LTag mouse monoclonal antibody Pab416 (red, Alexa Fluor 568). The DNA (nucleus) was stained with Draq5 (blue). Images were acquired by confocal microscopy with a 20× objective. Cells 3 days postseeding (A) and 3 days postinfection with BKPyV Dunlop (B).

Since SVG-A cells were found to be negative for BKPyV infection, we investigated whether the SVG-A cells represented a subpopulation of SVG with resistance to BKPyV infection. Therefore, SVG-A cells were seeded and infected by BKPyV (Dunlop). At 3 dpi, cells were fixed, and immunofluorescence staining was performed with polyclonal BKPyV agnoprotein antiserum. Microscopy revealed numerous BKPyV-infected cells (Fig. 6B). Thus, SVG-A cells do not contain BKPyV but are permissive for BKPyV infection.

## DISCUSSION

The SVG p12 cell line is one of few human cell lines available for propagation of JCPyV (6, 34). As such, a number of previous JCPyV studies, including drug efficacy studies (27, 36) as well as production of antigen for antibody detection assays (26), have utilized SVG or subclones of these cells. Moreover, SVG cells have been used in other settings where human glial cells are relevant, such as investigation of cerebral HIV replication (56).

We report here that the SVG p12 cell line as obtained directly from ATCC is productively infected with BKPyV. This infection, which has been undetected until now, may have influenced critical results of previous studies and must be taken into consideration in future studies utilizing these cells.

The lines of evidence supporting the presence of infectious BKPyV in the SVG p12 cell line are as follows. First, immunofluorescent staining of SVG p12 cells with antiserum directed against BKPyV agnoprotein, previously shown not to cross-react with SV40 or JCPyV agnoprotein, showed the characteristic cytoplasmic staining pattern seen in BKPyV-infected cells (45, 57). This result was confirmed in a separate laboratory and by Western blotting. Second, a high viral load was measured by qPCR targeting BKPyV-specific sequences within LTag in SVG p12 supernatants and directly in a vial from ATCC upon arrival in the laboratory. These results were also confirmed in a second laboratory. In total, 4 vials from two different lots tested positive. Third, the cells produced viral particles that were indistinguishable from the positive control by electron microscopy. Fourth, the virus was infectious, as demonstrated by immunofluorescent staining of RPTECs, the natural host cells for BKPyV, and Vero cells following exposure to SVG p12 supernatants. Finally, full-genome sequencing identified BKPyV in two separate laboratories using different methods for both initial amplification and sequencing reactions. Both laboratories converged on the same sequence, that of strain UT of BKPyV. Sequencing also showed a spectrum of defective mutants, some of which were DNase protected, i.e., likely encapsidated, characteristics both consistent with a cell culture origin of the viral DNA rather than typical PCR contamination. Based on these findings, we feel confident that a subpopulation of SVG p12 from ATCC is indeed productively infected with BKPyV UT strain.

While both NGS and conventional sequencing of the cloned long-range PCR product indicated that several variants with deletions in the coding region coexisted in the SVG p12 cell supernatant, only NGS detected the apparent dominant variants. These variants had an approximately 1,260-bp deletion in the VP2-VP3-VP1 region, which encompassed the target sequences used for long-range PCR prior to conventional sequencing (Fig. 3C and 4B). This result illustrates the advantages of using an unbiased amplification protocol. In addition, 4 distinct deletion mutants were identified by long-range PCR and conventional sequencing (Fig. 3C). Moreover, PCR of the EVGR and LVGR followed by gel electrophoresis showed a spectrum of different product sizes (Fig. 3D) confirming that SVG p12 cells produced a wide range of fragmented BKPyV genomes. Cloning and sequencing of more than 10 colonies from the long-range PCR would probably have confirmed this.

We cannot fully exclude that some of the fragmented genomes found are due to amplification artifacts caused, for instance, by generation of secondary structures during the amplification prior to pyrosequencing (58) or from the rolling-circle amplification (59). However, the observation of deletion mutants by different methods supports the notion of fragmented genomes.

It is unlikely that BKPyV carrying deletions removing more than 25% of the genome (Fig. 3C and 4B) would be independently infectious. Indeed, some of the fragmented genomes are also expected to be replication incompetent due to deletion of the origin of replication. This notion was indirectly substantiated in our work, as only full-length BKPyV UT replicated to high levels when the virus was passaged twice in RPTECs. In the context of the chronically infected LTag-producing SVG p12 cells, the defective viruses were probably supplied with the missing viral proteins in *trans* by coexisting and replicating complete virus. This phenomenon has previously been demonstrated for BKPyV (60) as well as for JCPyV (61, 62). It is also supported by our DNase treatment data, which suggest that the defective genomes were encapsidated. Perhaps generation of defective genomes was driven by constitutive SV40 LTag expression, as this protein is known to cause replicative stress and mitotic dysfunction leading to both structural and numerical chromosome instability (63). Whatever the mechanism, generation of defective mutants in polyomavirus cell culture has previously been observed and seems to depend on both host and viral factors (64, 65). Although the spectrum of defective mutants suggests that the infection is longstanding, it is no definitive proof.

When did BKPyV first enter the SVG p12 cell line? Was BKPyV already present in the fetal brain tissue when the SVG cell line was established in 1985, or did it enter later as a contamination of the cell line? There have been some reports of BKPyV in the central nervous system (CNS) of adults (66–70), and one group has reported finding BKPyV DNA in fetal brains (71). It is more likely, however, that BKPyV entered as a contamination of the cell line. Unfortunately, NCCR and full-genome sequencing shed little light on the origin of the contaminating virus, as BKPyV UT appears to be a relatively common variant, having been found in patient samples both in North Norway in 1990 (50) and in the United States in 2005 (51). Of note, this strain has also been used in several research labs (10, 46, 72–74). Although we cannot pinpoint the infection temporally, we can be certain that BKPyV has been present in the cells at least since 2006 based on ATCC records.

A comprehensive account of the possible implications for studies conducted in SVG cells is beyond the scope of this article. The studies running the greatest risk of erroneous results are those involving the closely related JCPyV. As shown here, overt BKPyV infection is not needed for JCPyV to infect and replicate in SVG p12 cells. For JCPyV replication, the most important characteristic of these cells is probably the high level of SV40 LTag expression. SV40 LTag has previously been shown to support JCPyV DNA replication (75). However, we did also find JCPyV- and BKPyV-coinfected cells, and BKPyV may have influenced the JCPyV rep-

lication in these cells. Also, infection of neighboring cells with BKPyV may have indirectly influenced JCPyV replication. Moreover, the high homology of the JCPyV and BKPyV genomes and their antigenic similarity, which is between 63 and 83% for the different proteins (76), may have led to false interpretation of viral protein and DNA levels. More unsettling is the use of viral antigens purified from SVG cells for diagnostic purposes (26). If the SVG cells used in this study were contaminated with BKPyV, it is highly likely that the purified viral particles contained a mixture of BKPyV and JCPyV antigens. Diagnostic tests based on such antigens would exhibit cross-reactivity to JCPyV- and BKPyV-reactive sera. Clearly, this would affect the antibody seroprevalence, which significantly differs between BKPyV and JCPyV.

That only a subpopulation of the SVG p12 cells expresses BKPyV proteins may suggest that the SVG p12 cell line is heterogeneous. This is supported by a recent study showing that SVG cells give rise to clonal cell lines with different phenotypes (34). We therefore speculate that subcloning of SVG p12 cells might give rise to uncontaminated cell lines. Importantly, we found that the SVG-A subclone was not infected by BKPyV, and the research performed in these cells therefore seems to be cleared from suspicion. It is not completely clear to us when this subclone was generated, nor do we know the details on how this was performed, but given their permissivity for JCPyV, the SVG-A cells may be a useful substitute for SVG p12 cells.

In conclusion, a subpopulation of SVG p12 cells from ATCC, has been productively infected with BKPyV UT and defective mutants at least since 2006. This may have affected previous studies in unknown ways. It is therefore crucial that investigators who have used these cells examine their cells for BKPyV and, if needed, reexamine their results carefully. Naturally, this must also be considered in all future experiments with these cells.

## ACKNOWLEDGMENTS

We thank Rainer Gosert, University of Basel, for performing confirmatory immunofluorescence staining.

The project was financially supported by the Northern Norway Regional Health Authority Medical Research Program.

## REFERENCES

1. **Rinaldo CH, Hirsch HH.** 2013. The human polyomaviruses: from orphans and mutants to patchwork family. APMIS **121:**681–684. http://dx.doi.org/10.1111/apm.12125.
2. **Padgett BL, Walker DL, ZuRhein GM, Eckroade RJ, Dessel BH.** 1971. Cultivation of papova-like virus from human brain with progressive multifocal leucoencephalopathy. Lancet **i:**1257–1260.
3. **Gardner SD, Field AM, Coleman DV, Hulme B.** 1971. New human papovavirus (B.K.) isolated from urine after renal transplantation. Lancet **i:**1253–1257.
4. **Chesters PM, Heritage J, McCance DJ.** 1983. Persistence of DNA sequences of BK virus and JC virus in normal human tissues and in diseased tissues. J. Infect. Dis. **147:**676–684. http://dx.doi.org/10.1093/infdis/147.4.676.
5. **Egli A, Infanti L, Dumoulin A, Buser A, Samaridis J, Stebler C, Gosert R, Hirsch HH.** 2009. Prevalence of polyomavirus BK and JC infection and replication in 400 healthy blood donors. J. Infect. Dis. **199:**837–846. http://dx.doi.org/10.1086/597126.
6. **Hirsch HH, Kardas P, Kranz D, Leboeuf C.** 2013. The human JC polyomavirus (JCPyV): virological background and clinical implications. APMIS **121:**685–727. http://dx.doi.org/10.1111/apm.12128.
7. **Rinaldo CH, Tylden GD, Sharma BN.** 2013. The human polyomavirus BK (BKPyV): virological background and clinical implications. APMIS **121:**728–745. http://dx.doi.org/10.1111/apm.12134.
8. **Cole CN.** 1996. Polyomavirinae: the viruses and their replication, p 1997–2025. *In* Fields BN, Knipe DM, Howley PM (ed), Fields virology, 3rd ed. Lippincott-Raven, Philadelphia, PA.
9. **Trowbridge PW, Frisque RJ.** 1995. Identification of three new JC virus proteins generated by alternative splicing of the early viral mRNA. J. Neurovirol. **1:**195–206. http://dx.doi.org/10.3109/13550289509113966.
10. **Abend JR, Joseph AE, Das D, Campbell-Cecen DB, Imperiale MJ.** 2009. A truncated T antigen expressed from an alternatively spliced BK virus early mRNA. J. Gen. Virol. **90:**1238–1245. http://dx.doi.org/10.1099/vir.0.009159-0.
11. **An P, Saenz Robles MT, Pipas JM.** 2012. Large T antigens of polyomaviruses: amazing molecular machines. Annu. Rev. Microbiol. **66:**213–236. http://dx.doi.org/10.1146/annurev-micro-092611-150154.
12. **Ahuja D, Saenz-Robles MT, Pipas JM.** 2005. SV40 large T antigen targets multiple cellular pathways to elicit cellular transformation. Oncogene **24:**7729–7745. http://dx.doi.org/10.1038/sj.onc.1209046.
13. **Tan CS, Broge TA, Jr, Seung E, Vrbanac V, Viscidi R, Gordon J, Tager AM, Koralnik IJ.** 2013. Detection of JC virus-specific immune responses in a novel humanized mouse model. PLoS One **8:**e64313. http://dx.doi.org/10.1371/journal.pone.0064313.
14. **Hirsch HH.** 2010. Polyoma and papilloma virus infections after hematopoietic stem cell or solid organ transplantation, p 465–482. *In* Bowden P, Ljungman P, Snydman DR (ed), Transplant infections, 3rd ed. Lippincott Williams & Wilkins, Philadelphia, PA.
15. **Low J, Humes HD, Szczypka M, Imperiale M.** 2004. BKV and SV40 infection of human kidney tubular epithelial cells in vitro. Virology **323:**182–188. http://dx.doi.org/10.1016/j.virol.2004.03.027.
16. **Bernhoff E, Gutteberg TJ, Sandvik K, Hirsch HH, Rinaldo CH.** 2008. Cidofovir inhibits polyomavirus BK replication in human renal tubular cells downstream of viral early gene expression. Am. J. Transplant. **8:**1413–1422. http://dx.doi.org/10.1111/j.1600-6143.2008.02269.x.
17. **Li R, Sharma BN, Linder S, Gutteberg TJ, Hirsch HH, Rinaldo CH.** 2013. Characteristics of polyomavirus BK (BKPyV) infection in primary human urothelial cells. Virology **440:**41–50. http://dx.doi.org/10.1016/j.virol.2013.01.024.
18. **Mesquita R, Bjorkholm M, Ekman M, Bogdanovic G, Biberfeld P.** 1996. Polyomavirus-infected oligodendrocytes and macrophages within astrocytes in progressive multifocal leukoencephalopathy (PML). APMIS **104:**153–160. http://dx.doi.org/10.1111/j.1699-0463.1996.tb00701.x.
19. **Broekema NM, Imperiale MJ.** 2012. Efficient propagation of archetype BK and JC polyomaviruses. Virology **422:**235–241. http://dx.doi.org/10.1016/j.virol.2011.10.026.
20. **Shaw G, Morse S, Ararat M, Graham FL.** 2002. Preferential transformation of human neuronal cells by human adenoviruses and the origin of HEK 293 cells. FASEB J. **16:**869–871.
21. **Major EO, Miller AE, Mourrain P, Traub RG, de Widt E, Sever J.** 1985. Establishment of a line of human fetal glial cells that supports JC virus multiplication. Proc. Natl. Acad. Sci. U. S. A. **82:**1257–1261. http://dx.doi.org/10.1073/pnas.82.4.1257.
22. **Gluzman Y, Sambrook JF, Frisque RJ.** 1980. Expression of early genes of origin-defective mutants of simian virus 40. Proc. Natl. Acad. Sci. U. S. A. **77:**3898–3902. http://dx.doi.org/10.1073/pnas.77.7.3898.
23. **Dowling-Warriner CV, Trosko JE.** 2000. Induction of gap junctional intercellular communication, connexin43 expression, and subsequent differentiation in human fetal neuronal cells by stimulation of the cyclic AMP pathway. Neuroscience **95:**859–868.
24. **Heron PM, Turchan-Cholewo J, Bruce-Keller AJ, Wilson ME.** 2009. Estrogen receptor alpha inhibits the estrogen-mediated suppression of HIV transcription in astrocytes: implications for estrogen neuroprotection in HIV dementia. AIDS Res. Hum. Retroviruses **25:**1071–1081. http://dx.doi.org/10.1089/aid.2009.0065.
25. **Fuente-Martin E, Garcia-Caceres C, Morselli E, Clegg DJ, Chowen JA, Finan B, Brinton RD, Tschop MH.** 2013. Estrogen, astrocytes and the neuroendocrine control of metabolism. Rev. Endocr. Metab. Disord. **14:**331–338. http://dx.doi.org/10.1007/s11154-013-9263-7.
26. **Frye S, Trebst C, Dittmer U, Petry H, Bodemer M, Hunsmann G, Weber T, Luke W.** 1997. Efficient production of JC virus in SVG cells and the use of purified viral antigens for analysis of specific humoral and cellular immune response. J. Virol. Methods **63:**81–92. http://dx.doi.org/10.1016/S0166-0934(96)02117-9.
27. **Jiang ZG, Cohen J, Marshall LJ, Major EO.** 2010. Hexadecyloxypropyl-cidofovir (CMX001) suppresses JC virus replication in human fetal brain SVG cell cultures. Antimicrob. Agents Chemother. **54:**4723–4732. http://dx.doi.org/10.1128/AAC.00837-10.

28. **Bofill-Mas S, Clemente-Casares P, Major EO, Curfman B, Girones R.** 2003. Analysis of the excreted JC virus strains and their potential oral transmission. J. Neurovirol. **9:**498–507. http://dx.doi.org/10.1080/13550280390218887.
29. **Brickelmaier M, Lugovskoy A, Kartikeyan R, Reviriego-Mendoza MM, Allaire N, Simon K, Frisque RJ, Gorelik L.** 2009. Identification and characterization of mefloquine efficacy against JC virus in vitro. Antimicrob. Agents Chemother. **53:**1840–1849. http://dx.doi.org/10.1128/AAC.01614-08.
30. **Sariyer IK, Saribas AS, White MK, Safak M.** 2011. Infection by agnoprotein-negative mutants of polyomavirus JC and SV40 results in the release of virions that are mostly deficient in DNA content. Virol. J. **8:**255. http://dx.doi.org/10.1186/1743-422X-8-255.
31. **Gasparovic ML, Maginnis MS, O'Hara BA, Dugan AS, Atwood WJ.** 2009. Modulation of PML protein expression regulates JCV infection. Virology **390:**279–288. http://dx.doi.org/10.1016/j.virol.2009.05.017.
32. **Dang X, Vidal JE, Oliveira AC, Simpson DM, Morgello S, Hecht JH, Ngo LH, Koralnik IJ.** 2012. JC virus granule cell neuronopathy is associated with VP1 C terminus mutants. J. Gen. Virol. **93:**175–183. http://dx.doi.org/10.1099/vir.0.037440-0.
33. **Nelson CD, Derdowski A, Maginnis MS, O'Hara BA, Atwood WJ.** 2012. The VP1 subunit of JC polyomavirus recapitulates early events in viral trafficking and is a novel tool to study polyomavirus entry. Virology **428:**30–40. http://dx.doi.org/10.1016/j.virol.2012.03.014.
34. **Ferenczy MW, Johnson KR, Steinberg SM, Marshall LJ, Monaco MC, Beschloss AM, Jensen PN, Major EO.** 2013. Clonal immortalized human glial cell lines support varying levels of JC virus infection due to differences in cellular gene expression. J. Neuroimmune Pharmacol. **8:**1303–1319. http://dx.doi.org/10.1007/s11481-013-9499-8.
35. **Goldmann C, Petry H, Frye S, Ast O, Ebitsch S, Jentsch KD, Kaup FJ, Weber F, Trebst C, Nisslein T, Hunsmann G, Weber T, Luke W.** 1999. Molecular cloning and expression of major structural protein VP1 of the human polyomavirus JC virus: formation of virus-like particles useful for immunological and therapeutic studies. J. Virol. **73:**4465–4469.
36. **Hou J, Major EO.** 1998. The efficacy of nucleoside analogs against JC virus multiplication in a persistently infected human fetal brain cell line. J. Neurovirol. **4:**451–456. http://dx.doi.org/10.3109/13550289809114545.
37. **Qu Q, Sawa H, Suzuki T, Semba S, Henmi C, Okada Y, Tsuda M, Tanaka S, Atwood WJ, Nagashima K.** 2004. Nuclear entry mechanism of the human polyomavirus JC virus-like particle: role of importins and the nuclear pore complex. J. Biol. Chem. **279:**27735–27742.
38. **Orba Y, Suzuki T, Makino Y, Kubota K, Tanaka S, Kimura T, Sawa H.** 2010. Large T antigen promotes JC virus replication in G2-arrested cells by inducing ATM- and ATR-mediated G2 checkpoint signaling. J. Biol. Chem. **285:**1544–1554. http://dx.doi.org/10.1074/jbc.M109.064311.
39. **Wang M, Tsou TH, Chen LS, Ou WC, Chen PL, Chang CF, Fung CY, Chang D.** 2004. Inhibition of simian virus 40 large tumor antigen expression in human fetal glial cells by an antisense oligodeoxynucleotide delivered by the JC virus-like particle. Hum. Gene Ther. **15:**1077–1090. http://dx.doi.org/10.1089/hum.2004.15.1077.
40. **Pho MT, Ashok A, Atwood WJ.** 2000. JC virus enters human glial cells by clathrin-dependent receptor-mediated endocytosis. J. Virol. **74:**2288–2292. http://dx.doi.org/10.1128/JVI.74.5.2288-2292.2000.
41. **Zins SR, Nelson CD, Maginnis MS, Banerjee R, O'Hara BA, Atwood WJ.** 2014. The human alpha defensin HD5 neutralizes JC polyomavirus infection by reducing endoplasmic reticulum traffic and stabilizing the viral capsid. J. Virol. **88:**948–960. http://dx.doi.org/10.1128/JVI.02766-13.
42. **Schweighardt B, Shieh JT, Atwood WJ.** 2001. CD4/CXCR4-independent infection of human astrocytes by a T-tropic strain of HIV-1. J. Neurovirol. **7:**155–162. http://dx.doi.org/10.1080/13550280152058816.
43. **Rinaldo CH, Gosert R, Bernhoff E, Finstad S, Hirsch HH.** 2010. 1-O-hexadecyloxypropyl cidofovir (CMX001) effectively inhibits polyomavirus BK replication in primary human renal tubular epithelial cells. Antimicrob. Agents Chemother. **54:**4714–4722. http://dx.doi.org/10.1128/AAC.00974-10.
44. **Hey AW, Johnsen JI, Johansen B, Traavik T.** 1994. A two fusion partner system for raising antibodies against small immunogens expressed in bacteria. J. Immunol. Methods **173:**149–156. http://dx.doi.org/10.1016/0022-1759(94)90294-1.
45. **Rinaldo CH, Traavik T, Hey A.** 1998. The agnogene of the human polyomavirus BK is expressed. J. Virol. **72:**6233–6236.
46. **Rinaldo CH, Myhre MR, Alstad H, Nilssen O, Traavik T.** 2003. Human polyomavirus BK (BKV) transiently transforms and persistently infects cultured osteosarcoma cells. Virus Res. **93:**181–187. http://dx.doi.org/10.1016/S0168-1702(03)00096-0.
47. **Dumoulin A, Hirsch HH.** 2011. Reevaluating and optimizing polyomavirus BK and JC real-time PCR assays to detect rare sequence polymorphisms. J. Clin. Microbiol. **49:**1382–1388. http://dx.doi.org/10.1128/JCM.02008-10.
48. **Agostini HT, Stoner GL.** 1995. Amplification of the complete polyomavirus JC genome from brain, cerebrospinal fluid and urine using pre-PCR restriction enzyme digestion. J. Neurovirol. **1:**316–320. http://dx.doi.org/10.3109/13550289509114028.
49. **Olsen GH, Hirsch HH, Rinaldo CH.** 2009. Functional analysis of polyomavirus BK non-coding control region quasispecies from kidney transplant recipients. J. Med. Virol. **81:**1959–1967. http://dx.doi.org/10.1002/jmv.21605.
50. **Sundsfjord A, Johansen T, Flaegstad T, Moens U, Villand P, Subramani S, Traavik T.** 1990. At least two types of control regions can be found among naturally occurring BK virus strains. J. Virol. **64:**3864–3871.
51. **Sharma PM, Gupta G, Vats A, Shapiro R, Randhawa P.** 2006. Phylogenetic analysis of polyomavirus BK sequences. J. Virol. **80:**8869–8879. http://dx.doi.org/10.1128/JVI.00510-06.
52. **Gee GV, Manley K, Atwood WJ.** 2003. Derivation of a JC virus-resistant human glial cell line: implications for the identification of host cell factors that determine viral tropism. Virology **314:**101–109. http://dx.doi.org/10.1016/S0042-6822(03)00389-1.
53. **Orba Y, Sawa H, Iwata H, Tanaka S, Nagashima K.** 2004. Inhibition of virus production in JC virus-infected cells by postinfection RNA interference. J. Virol. **78:**7270–7273. http://dx.doi.org/10.1128/JVI.78.13.7270-7273.2004.
54. **Ashok A, Atwood WJ.** 2003. Contrasting roles of endosomal pH and the cytoskeleton in infection of human glial cells by JC virus and simian virus 40. J. Virol. **77:**1347–1356. http://dx.doi.org/10.1128/JVI.77.2.1347-1356.2003.
55. **Querbes W, Benmerah A, Tosoni D, Di Fiore PP, Atwood WJ.** 2004. A JC virus-induced signal is required for infection of glial cells by a clathrin- and eps15-dependent pathway. J. Virol. **78:**250–256. http://dx.doi.org/10.1128/JVI.78.1.250-256.2004.
56. **Schweighardt B, Atwood WJ.** 2001. HIV type 1 infection of human astrocytes is restricted by inefficient viral entry. AIDS Res. Hum. Retroviruses **17:**1133–1142. http://dx.doi.org/10.1089/088922201316912745.
57. **Unterstab G, Gosert R, Leuenberger D, Lorentz P, Rinaldo CH, Hirsch HH.** 2010. The polyomavirus BK agnoprotein co-localizes with lipid droplets. Virology **399:**322–331. http://dx.doi.org/10.1016/j.virol.2010.01.011.
58. **Vandenbroucke I, Van Marck H, Verhasselt P, Thys K, Mostmans W, Dumont S, Van Eygen V, Coen K, Tuefferd M, Aerssens J.** 2011. Minor variant detection in amplicons using 454 massive parallel pyrosequencing: experiences and considerations for successful applications. Biotechniques **51:**167–177.
59. **Wang Y, Lee OO, Yang JK, Li TG, Qian PY.** 2013. Artifactual pyrosequencing reads in multiple-displacement-amplified sediment metagenomes from the Red Sea. PeerJ **1:**e69. http://dx.doi.org/10.7717/peerj.69.
60. **Myhre MR, Olsen GH, Gosert R, Hirsch HH, Rinaldo CH.** 2010. Clinical polyomavirus BK variants with agnogene deletion are nonfunctional but rescued by trans-complementation. Virology **398:**12–20. http://dx.doi.org/10.1016/j.virol.2009.11.029.
61. **Yoshiike K, Miyamura T, Chan HW, Takemoto KK.** 1982. Two defective DNAs of human polyomavirus JC adapted to growth in human embryonic kidney cells. J. Virol. **42:**395–401.
62. **Mandl C, Walker DL, Frisque RJ.** 1987. Derivation and characterization of POJ cells, transformed human fetal glial cells that retain their permissivity for JC virus. J. Virol. **61:**755–763.
63. **Hu L, Filippakis H, Huang H, Yen TJ, Gjoerup OV.** 2013. Replication stress and mitotic dysfunction in cells expressing simian virus 40 large T antigen. J. Virol. **87:**13179–13192. http://dx.doi.org/10.1128/JVI.02224-13.
64. **O'Neill FJ, Carroll D.** 1983. Role of defective simian virus 40 genomes in establishment and maintenance of persistently infected primate cell lines. Intervirology **19:**181–194.
65. **Martin JD, Padgett BL, Walker DL.** 1983. Characterization of tissue culture-induced heterogeneity in DNAs of independent isolates of JC virus. J. Gen. Virol. **64**(Part 10)**:**2271–2280. http://dx.doi.org/10.1099/0022-1317-64-10-2271.
66. **Jorgensen GE, Hammarin AL, Bratt G, Grandien M, Flaegstad T, Johnsen JI.** 2003. Identification of a unique BK virus variant in the CNS of

a patient with AIDS. J. Med. Virol. **70:**14–19. http://dx.doi.org/10.1002/jmv.10370.

67. **Barcena-Panero A, Echevarria JE, Van Ghelue M, Fedele G, Royuela E, Gerits N, Moens U.** 2012. BK polyomavirus with archetypal and rearranged non-coding control regions is present in cerebrospinal fluids from patients with neurological complications. J. Gen. Virol. **93:**1780–1794. http://dx.doi.org/10.1099/vir.0.042143-0.
68. **Vidal JE, Fink MC, Cedeno-Laurent F, Delbue S, Ferrante P, Dauar RF, Filho FB, Nogueira RS, Calore EE, Pannuti CS, Trujillo JR, de Oliveira AC.** 2007. BK virus associated meningoencephalitis in an AIDS patient treated with HAART. AIDS Res. Ther. **4:**13. http://dx.doi.org/10.1186/1742-6405-4-13.
69. **Stoner GL, Alappan R, Jobes DV, Ryschkewitsch CF, Landry ML.** 2002. BK virus regulatory region rearrangements in brain and cerebrospinal fluid from a leukemia patient with tubulointerstitial nephritis and meningoencephalitis. Am. J. Kidney Dis. **39:**1102–1112. http://dx.doi.org/10.1053/ajkd.2002.32795.
70. **Elsner C, Dorries K.** 1992. Evidence of human polyomavirus BK and JC infection in normal brain tissue. Virology **191:**72–80. http://dx.doi.org/10.1016/0042-6822(92)90167-N.
71. **Boldorini R, Allegrini S, Miglio U, Nestasio I, Paganotti A, Veggiani C, Monga G, Pietropaolo V.** 2010. BK virus sequences in specimens from aborted fetuses. J. Med. Virol. **82:**2127–2132. http://dx.doi.org/10.1002/jmv.21923.
72. **Abend JR, Low JA, Imperiale MJ.** 2007. Inhibitory effect of gamma interferon on BK virus gene expression and replication. J. Virol. **81:**272–279. http://dx.doi.org/10.1128/JVI.01571-06.
73. **Chen PL, Hsu PH, Fang CY, Chang CF, Ou WC, Wang M, Chang D.** 2011. Phosphorylation of Ser-80 of VP1 and Ser-254 of VP2 is essential for human BK virus propagation in tissue culture. J. Gen. Virol. **92:**2637–2645. http://dx.doi.org/10.1099/vir.0.033282-0.
74. **Fang CY, Chen HY, Wang M, Chen PL, Chang CF, Chen LS, Shen CH, Ou WC, Tsai MD, Hsu PH, Chang D.** 2010. Global analysis of modifications of the human BK virus structural proteins by LC-MS/MS. Virology **402:**164–176. http://dx.doi.org/10.1016/j.virol.2010.03.029.
75. **Nesper J, Smith RW, Kautz AR, Sock E, Wegner M, Grummt F, Nasheuer HP.** 1997. A cell-free replication system for human polyomavirus JC DNA. J. Virol. **71:**7421–7428.
76. **Rekvig OP, Bendiksen S, Moens U.** 2006. Immunity and autoimmunity induced by polyomaviruses: clinical, experimental and theoretical aspects. Adv. Exp. Med. Biol. **577:**117–147. http://dx.doi.org/10.1007/0-387-32957-9_9.
77. **Chen Y, Sharp PM, Fowkes M, Kocher O, Joseph JT, Koralnik IJ.** 2004. Analysis of 15 novel full-length BK virus sequences from three individuals: evidence of a high intra-strain genetic diversity. J. Gen. Virol. **85:**2651–2663. http://dx.doi.org/10.1099/vir.0.79920-0.
78. **Sundsfjord A, Spein AR, Lucht E, Flaegstad T, Seternes OM, Traavik T.** 1994. Detection of BK virus DNA in nasopharyngeal aspirates from children with respiratory infections but not in saliva from immunodeficient and immunocompetent adult patients. J. Clin. Microbiol. **32:**1390–1394.